

Development of Analytical Models to Estimate Pile Setup in Cohesive Soils Based on FE Numerical Analyses

Firouz Rosti · Murad Abu-Farsakh ·
Jongwon Jung

Received: 8 February 2016 / Accepted: 17 May 2016 / Published online: 24 May 2016
© Springer International Publishing Switzerland 2016

Abstract This paper presents the numerical simulation of pile installation and the subsequent increase in the pile capacity over time (or setup) after installation that was performed using the finite element software Abaqus. In the first part, pile installation and the following load tests were simulated numerically using the volumetric cavity expansion concept. The anisotropic modified Cam-Clay and Drucker–Prager models were adopted in the FE model to describe the behavior of the clayey and sandy soils, respectively. The proposed FE model proposed was successfully validated through simulating two full-scale instrumented driven pile case studies. In the second part, over 100 different actual properties of individual soil layers distracted from literature were used in the finite element analysis to conduct parametric study and to evaluate the effect of different soil properties on the pile setup behavior. The setup factor A was targeted here to describe the pile setup as a function of time after the end of driving. The selected soil properties in this study to evaluate the setup factor A include: soil plasticity index (PI), undrained shear strength (S_u),

vertical coefficient of consolidation (C_v), sensitivity ratio (S_r), and over-consolidation ratio (OCR). The predicted setup factor showed direct proportion with the PI and S_r and inverse relation with S_u , C_v , and OCR. These soil properties were selected as independent variables, and nonlinear multivariable regression analysis was performed using Gauss–Newton algorithm to develop appropriate regression models for A . Best models were selected among all based on level of errors of prediction, which were validated with additional nineteen different site information available in the literature. The results indicated that the developed model is able to predict the setup behavior for individual cohesive soil layers, especially for values of setup factor greater than 0.10, which is the most expectable case in nature.

Keywords Numerical modeling · Pile setup · Regression analysis

1 Introduction

During pile driving, the adjacent soil usually disturbs and remolds, and excess porewater pressures develops within influence zone, especially for piles driven in saturated cohesive soils. The induced excess porewater pressure tends to dissipate over time and the soil particles begins to rearrange resulting in an increase in the soil shear strength over time after end of pile

F. Rosti · J. Jung
Department of Civil and Environmental Engineering,
Louisiana State University, Baton Rouge, LA 70803, USA

M. Abu-Farsakh (✉)
Louisiana Transportation Research Center, Louisiana
State University, 4101 Gourrier Ave, Baton Rouge,
LA 70808, USA
e-mail: cefars@lsu.edu

driving. The increase in pile capacity over time in driven piles is related to the dissipation of the excess porewater pressure (consolidation), the soil strength regaining with time at constant stress state (thixotropic behavior), and the change in soil fabrics as well as creep effects at time after consolidation (aging). Salgado (2008) indicated that the pile setup is mostly due to the dissipation of excess porewater pressure (consolidation) and the strength regaining of remolded soil near piles over time (thixotropy). Thixotropy is defined by Mitchell (1960) as the “process of softening caused by remolding, followed by a time-dependent return to the original harder state”. The fine-grained cohesive soils show certain degree of thixotropic response under constant effective stress and constant void ratio. Thixotropy is a reversible process, which is mainly related to the rearrangement of the remolded soil particles and regaining of soil bounding, that must be considered in constitutive models that simulate with shear failure at the soil-structure interface such as driven piles, and the following increase in pile capacity with time (or pile setup) after end of driving (EOD). Abu-Farsakh et al. (2015) introduced a rational relation for soil disturbance during pile installation and the following construction and thixotropic responses.

The combination of consolidation, thixotropic and aging increase in pile capacity is referred as setup or freeze (Titi and Wathugala 1999). The term “setup” have been used in the literature to describe this phenomenon of time-dependent capacity increase (e.g., Randolph and Wroth 1979; Bullock et al. 2005; Fakharian et al. 2013). The setup phenomenon is evaluated using a term called setup factor A , which was introduced by Skov and Denver (1988), and indicates the rate of increase in pile capacity over time follows a logarithmic trend. Performing extensive and expensive full-scale pile instrumentation and the following static or dynamic load tests is being a common practice to study the soil setup behavior over time (e.g. Konard and Roy 1987; Karlsrud et al. 2005; Khan and Decapite 2011; Bullock et al. 2005; Hauqe et al. 2014). Beside experimental study, some researchers have attempted to relate soil setup to soil properties of a specific location (e.g. Karlsrud et al. 2005; Ng 2011; Ng et al. 2013; Hauqe et al. 2016). Plenty of databases from previous experimental studies on soil setup are available in literature, which are being used to quantify the pile setup using statistical

regression analysis (Karlsrud et al. 2005; Ng et al. 2013; Hauqe et al. 2016).

Researchers attempted to investigate pile setup by using appropriate numerical simulation (e.g., Wathugala 1990; Titi and Wathugala 1999; Elias 2008; Chakraborty et al. 2013; Abu-Farsakh et al. 2015). Pile installation can be simulated numerically by creating a volumetric cavity equal to the pile size through applying prescribed displacement to the soil boundary points, and then displacing pile inside the cavity and activating soil-pile interface interaction (Abu-Farsakh et al. 2003; Rosti and Abu-Farsakh 2015). In most of these studies, cavity expansion theory has been used to establish pile penetration; the theory of consolidation has been applied to model dissipation of excess porewater pressure. Finally, vertical shear load has been applied at different times after EOD to estimate the setup (e.g., Abu-Farsakh et al. 2015; Titi and Wathugala 1999; Rosti and Abu-Farsakh 2015; Augustesen 2006; Elias 2008; Fakharian et al. 2013).

In this study, the Abaqus software and the numerical techniques as described in Abu-Farsakh et al. (2015) were used, and numerical simulations were conducted to model pile penetration in soil body. The soil thixotropic behavior was implemented in numerical model using the formulation proposed by Abu-Farsakh et al. (2015). In this paper, a full-scale instrumented pile installed in clayey soil at Bayou Zouri Bridge site in Louisiana and the following load tests were first simulated for verification and validation of the finite elements (FE) model. In order to perform parametric study, the soil information for over 100 individual soil layers were collected from Louisiana and nationwide for use as input data in the numerical simulation. The properties of the specified soils were used in numerical simulation and the corresponding predicted setup factor A for each soil layer was obtained. To develop a rational relation between A and soil properties, the multivariable nonlinear regression analysis was conducted on the results of FE analysis and the obtained setup factor values using Gauss–Newton algorithm, which is available in statistical analysis system (SAS) software.

2 Description of Test Site

The simulated case study project consists of constructing a two-lane highway bridge on the northbound

lane of U.S.171 over Bayou Zouri in Vernon Parish of Louisiana. The existing bridge required replacement due to substandard load carrying capacity and the embankment protection is severely undetermined. A square prestressed precast concrete (PPC) pile foundation having a width of 61 cm were selected to support the bridge structure. One pile with a 16.8 m embedded length was selected to perform two static load tests (SLT) and four dynamic load tests (DLT) to study the setup behavior over a period of 77 days from EOD. The ground water level was located at about one meter below the ground surface. The subsurface soil was characterized using in situ standards penetration test (SPT), cone penetration test (CPT), and piezocone penetration test (PCPT). The research team also performed laboratory soil tests on undisturbed soil samples, such as triaxial tests and consolidation tests. The subsurface soil is mainly consists of stiff clay with some loose sandy soil interlayers located in the top 10 m below the ground surface. The SPT number of the sand layers varies from 2 to 25 and the undrained shear strength (S_u) of the clay layers ranges from 138 to 342 kPa (from UU test) and 151 to 488 kPa, which was estimated from the CPT data using a N_K (empirical cone factor) value of 15 (Chen et al. 2014). The values of horizontal coefficient of consolidation (C_h) were estimated from the piezometer dissipation tests using the Teh and Houlsby method (1991). In this paper, the C_h values were converted to the horizontal coefficient of consolidation (C_v) and presented in text in order to keep compatibility between data.

3 Finite Element Numerical Modeling

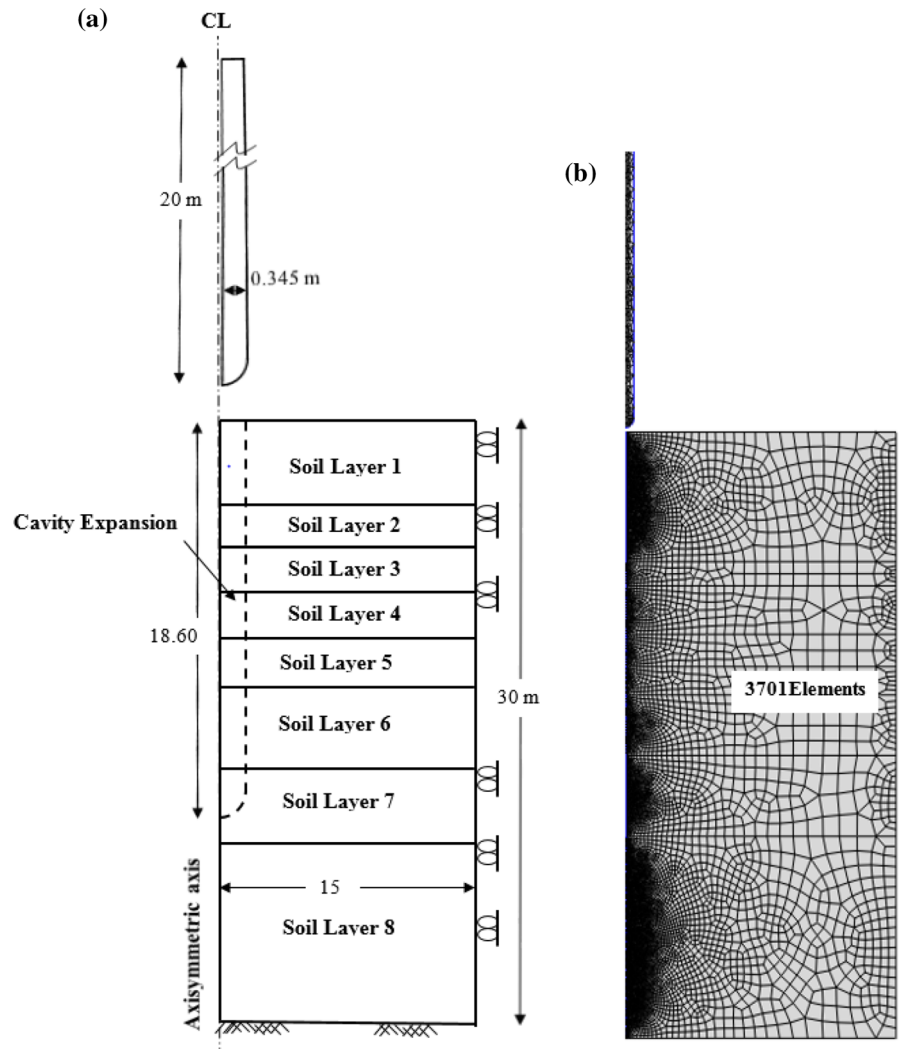
In this study, two square PPC test piles driven in Bayou Zouri Bridge and Bayou Lacassine sites were modeled using FE numerical analysis. The test piles were fully instrumented with strain gages, piezometers and load cells installed at different depths along the pile length. The piles have square cross sections; however, an equivalent circular shape was adopted in this study to ease the FE modeling of the cavity expansion. The FE software Abaqus was used for numerical modeling. The geometry of soil and pile and the applied boundary conditions for Bayou Zouri site and the corresponding soil layering are shown in Fig. 1. As indicated in this figure, a fixed boundary condition was applied to the soil bottom, all degrees of

freedom of left and right soil boundary were constrained except the vertical displacement, and the soil top surface was left free to move in the vertical direction. Water was allowed to flow in the soil top surface. A curved shape was adopted for the pile tip to minimize the effect of sharp corner complexity in the numerical solution. Linear quadrilateral coupled pore-water elements were selected for the whole soil domain to avoid shear locking and provide more accurate results than other elements (Shao 1998; Walker and Yu 2006).

The pile installation was modeled by the combination of volumetric cavity expansion followed by applying vertical shear displacement (penetration) in an axisymmetric FE model. The theory of consolidation followed by the shearing at pile-soil interface was used to model the pile setup phenomenon. In this model, geostatic step was applied to the whole soil body in order to achieve initial equilibrium condition (step1); series of prescribed displacement in the soil's axisymmetric boundary were then applied (step 2) to create a displaced volume equal to the size of the pile (volumetric cavity expansion, Abu-Farsakh et al. 2003). The pile was then placed inside the cavity, and the interaction between the pile and soil surrounding soil was activated (step 3). The prescribed boundary conditions to create cavity expansion were released, and an additional vertical penetration step was applied incrementally (initial shear step, step 4) until the steady state condition is reached. This step provides pore water pressure generation around the pile tip, which was not mobilized appropriately during the second step. Figure 2a, b present the developed total porewater pressure distribution around the pile tip before and after the initial shear step 4, respectively. These figures were obtained from the numerical simulation and show that the porewater pressure values beneath the pile tip are increased from 50 kPa before the initial shear step to reach 800 kPa after this step. The developed excess porewater pressure during the installation was allowed to dissipate for different elapsed time after installation to simulate static load tests at different times (step 5). The static load test was then simulated by applying an additional penetration to pile and hence additional vertical shear displacement at the interface until failure (final shear step, step 6).

In this study, the surface to surface master–slave contact model was used to simulate the pile-soil interface friction. The contact between the two

Fig. 1 Numerical simulation domain: **a** geometry and boundary conditions, **b** FE mesh



surfaces are controlled by kinematic constraints in the normal and tangential directions. When the pile is in contact with the soil, the normal stress at contact is compressive, and it is zero when there is gap between the pile and the soil. The Coulomb frictional contact law was used to model the frictional sliding at the pile-soil interface.

4 Constitutive Model

The anisotropic modified cam-clay (AMCC) model and Drucker–Prager (DP) model were adopted to describe the behavior of clayey and sandy soils,

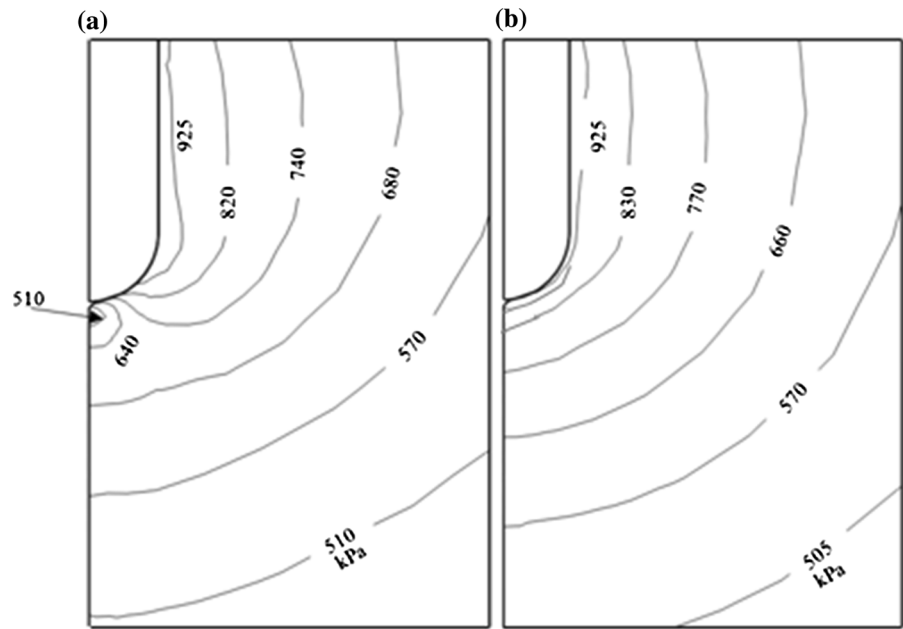
respectively. The AMCC model was implemented via UMAT in the Abaqus software to describe the behavior of saturated cohesive soils. Equations (1) and (2) introduce the yield surface for AMCC and DP models in $q - p$ space, respectively:

$$f = p^2 - pp_0 + \frac{1}{M^2} (q^2 - 2\alpha pq + \alpha^2 pp_0) = 0 \quad (1)$$

$$f = q - p \tan \beta^* - d = 0 \quad (2)$$

In Eqs. (1) and (2), $p = \frac{1}{3} \text{trace}(\sigma_{ij})$ is the effective hydrostatic stress, $q = \sqrt{S_{ij}S_{ij}}$ is equivalent deviatoric stress in which S_{ij} is the deviatoric part of stress tensor σ_{ij} . P_0 is the pre-consolidation stress, M is the critical

Fig. 2 Porewater pressure mobilization during initial shear step beneath the pile tip: **a** before initial shear, **b** after initial shear



state parameter, which is the slope of the critical state line (CSL), α is a non-dimensional anisotropic variable, β^* represents the soil friction angle in DP model, and d is parameter related to the soil cohesion. β^* and d , respectively, are related to the soil internal friction angle, Φ , and soil cohesion, c , with the following equations:

$$\beta^* = \tan^{-1} \left(\frac{2 \sin \Phi}{\sqrt{3}(3 - \sin \Phi)} \right) \tag{3}$$

$$d = \frac{6c \cos \Phi}{\sqrt{3}(3 - \sin \Phi)} \tag{4}$$

Figure 3a, b depict the graphical representation for AMCC and DP models, respectively. Detailed discussion about AMCC model is available in the literature (e.g., Dafalias 1987; Abu-Farsakh et al. 2015). Since for the PPC piles driven under satisfactory drivability criteria, the pile deformation is insignificant and usually stays within the elastic range in comparison to the adjacent soil; therefore, an elastic model was adopted to model the pile. The pile unit weight was selected to be 20 kN/m³, and the Poisson ratio and Young’s modulus values of 0.20 and 20 GPa, respectively, were adopted. Based on the soil profile obtained from in situ PCPT, the subsurface soil was divided into

Fig. 3 Graphical representation of yield surface for: **a** AMCC model and **b** DP model

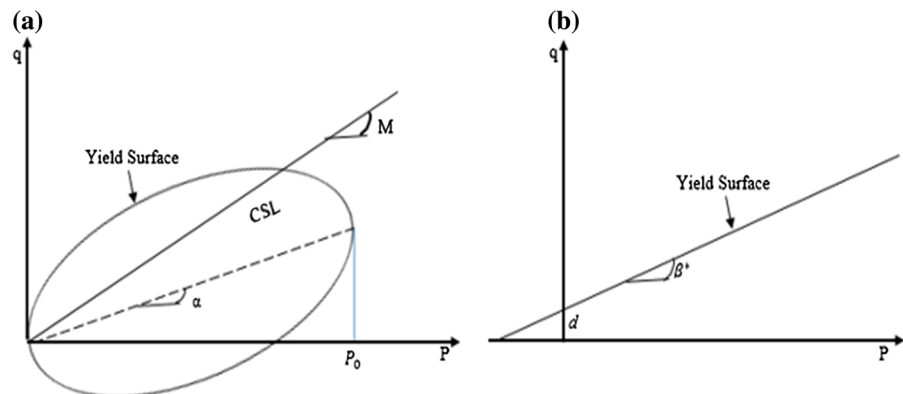


Table 1 Soil material parameters for the test pile in Bayou Zouri Bridge site

Layer no.	Soil type	Depth (m)	w (%)	e_0	K_0	S_u (kPa)	M	λ	κ	OCR	K (m/s) 10^{-9}	β^*
1	Sand	0–4.7	23	0.6	1.19	–	–	–	–	–	310	4530
2	Sand	4.7–6	32	0.8	1.15	–	–	–	–	–	230	4770
3	Sand	6–8.6	32	0.8	1.16	–	–	–	–	–	150	4714
4	Clay	8.6–10.3	29	0.7	1.18	150	1.48	0.11	0.02	3.50	0.595	–
5	Clay	10.3–12	21	0.5	1.10	138	0.90	0.12	0.02	2.50	0.137	–
6	Clay	12–15	28	0.8	0.90	350	0.90	0.15	0.03	2	0.398	–
7	Clay	15–18	23	0.6	0.60	390	0.86	0.17	0.03	1	0.483	–
8	Clay	18–30	23	0.6	0.60	390	0.86	0.17	0.03	1	0.483	–

eight soil layers for the test pile. Tables 1 represents the soil layering, soil properties and model parameters used in the FE numerical simulation. In this table, w is the soil water content; λ and κ are the loading and unloading slope, respectively; e_0 , K_0 , OCR and K are the initial void ratio, lateral earth pressure coefficient at rest, over-consolidation ratio and hydraulic conductivity for each soil layers, respectively.

5 Soil Thixotropic Behavior

Fine-grained cohesive soils show degrees of thixotropic response under constant effective stress and constant void ratio. In order to conduct numerical study of the pile installation and the following setup phenomenon, both consolidation and thixotropic behaviors in cohesive soil should be considered. For driven piles, which deal with change in the soil properties during different steps of installation and the following setup, adopting the material properties for numerical study is a challenging task. Therefore, numerical simulation of pile setup using properties obtained from laboratory tests like triaxial or consolidation tests on undisturbed soil samples yields unrealistic results. In this paper, a time-dependent strength reduction parameter $\beta(t)$ was applied to the strength parameter M as well as the pile-soil interface friction coefficient μ , similar to the work done by Fakharian et al. (2013) and Abu-Farsakh et al. (2015), to incorporate effect of soil remolding during pile installation:

$$\begin{cases} M(t) = \beta(t)M \\ \mu(t) = \beta(t)\mu \end{cases} \quad (5)$$

An evolution function was then proposed to capture the strength increase over time for the remolded soil

around the pile. Equation 6 presents this time-dependent function and its evolution with time, which was deployed from similar research on thixotropic behavior of inks addresses in Barnes (1997).

$$\beta(t) = \beta(\infty) - [\beta(\infty) - \beta(0)]e^{-\frac{t}{\tau}} \quad (6)$$

where $\beta(0)$ is the initial value for reduction parameter β for the time t immediately after pile installation, which is usually related to the soil sensitivity, and $\beta(\infty)$ represents the β value after a long time from soil disturbance. Information regarding the soil sensitivity for the test sites were not available; however, based on the study that was performed on another test site with similar soil condition in Louisiana, a value of $\beta(0) = 0.75$ was reasonably adopted this site. This value for $\beta(0)$ is obtained from $\beta(0) = (S_r)^{-0.3}$ with adopting sensitivity value equal to 3. Detailed description regarding the thixotropy formulation in pile installation and setup is available in Abu-Farsakh et al. (2015).

For naturally non-structured soils with low sensitivity, long-term strength regaining during thixotropic behavior might be equal to the undisturbed strength values. On the other hand, $\beta(\infty)$ can be 1 for low sensitive clay (as adopted here) and it can be reached a value greater than 1 for soils with artificially structured with cement slurry or salt after remolding. In Eq. 6, τ is a time constant and it can be defined in relation to t_{90} , which is the time for 90 % dissipation of the excess pore water pressure at the pile surface. More investigation is required to find real value for τ ; however, in this study it was simply assumed that $\tau = t_{90}$. Values for t_{90} were derived from PCPT dissipation test curves using Teh and Houlsby (1991) method.

6 Verification of FE Model

6.1 Case Study 1 (Bayou Zouri Bridge Site)

The pile installation usually results in the development of excess porewater pressure, which dissipates with time after EOD. In numerical simulation, the coupled pore pressure analysis provides porewater generation and its dissipation with time. The change in excess pore water pressure with time after EOD for the Bayou Zouri Bridge site, which obtained from field test measurements through the piezometers installed on the pile face, and the corresponding numerical simulation values are presented in Fig. 4a, b for the two depths 7.60 and 10.70 m, respectively, corresponds to soil layers three and five. These figures demonstrate good agreement between the field measurement and results of FE numerical simulation.

The increase in the pile shaft resistance over time after EOD obtained from the field load tests and the corresponding values predicted from numerical simulation are presented in Fig. 5. The field results for the site were obtained from both the SLT and DLT results. Figure 5 shows that the predicted shaft resistances using FE numerical simulation (Dashed line) overestimates the pile shaft resistance for a short time after EOD, and then reach the field measured values after a long time, at about 100 days after EOD for this site.

This observation can be explained by the disturbance that occurs at the pile-soil interface during pile installation and the effect of thixotropic behavior of the soil in regaining its strength with time. For accurate prediction, numerical simulation was re-performed using reduced properties for remolded soil strength ($\beta(t = 0) = 0.75$) starting immediately after EOD, and then adjusting the properties to capture the soil thixotropic response with time after EOD ($\beta(t = t_{90}) = 1$). The predicted results by including the soil thixotropic response are shown in Fig. 5 with solid line. The response predicted by considering soil disturbance during pile installation and the thixotropic behavior after that demonstrated better agreement with the measured results from field tests. In this figure, the SLT pile capacity results obtained using Davisson interpolation method for piles, showed over prediction of pile capacity in comparison with the results obtained from DLTs and numerical simulation.

6.2 Case Study 2 (Bayou Lacassine Bridge Site)

Using the described FE model, the authors simulated three full-scale instrumented driven piles in Bayou Lacassine, Louisiana. Detailed description of the test site including geometries of the piles and soil, FE model, FE predicted pile capacities, and analyses are available in Abu-Farsakh et al. (2015). However, this

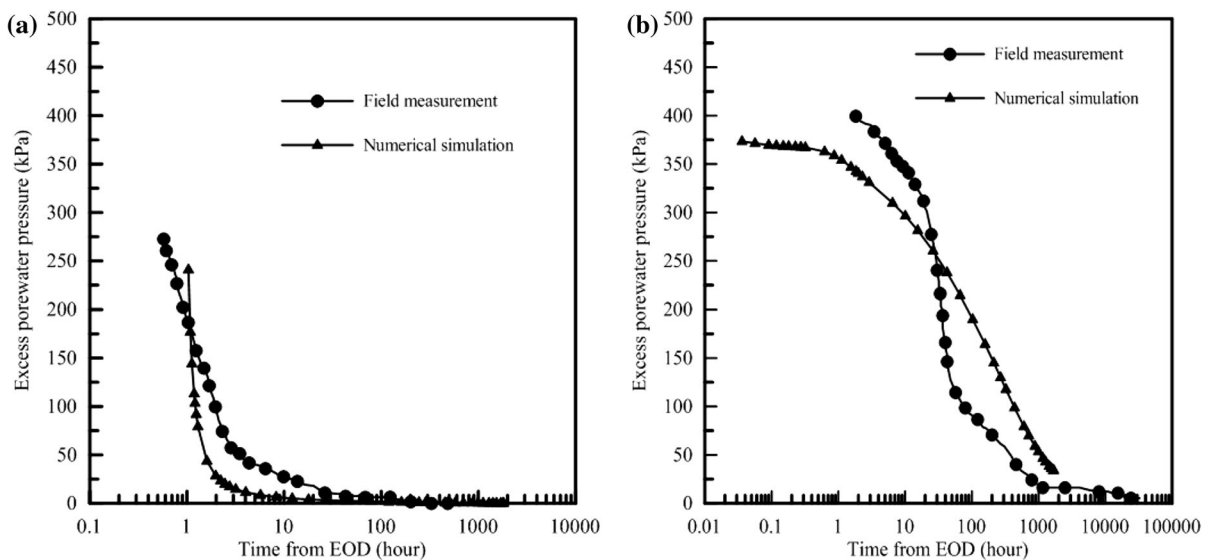


Fig. 4 Comparison between the numerical and measured excess pore water pressure dissipation with time after EOD obtained at different depths: **a** at $Z = 7.60$ m, and **b** at $Z = 10.70$ m

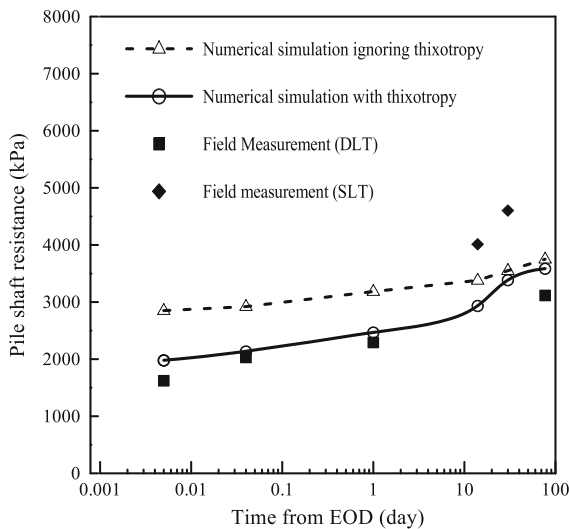


Fig. 5 Increase in pile shaft resistance with time after EOD for Bayou Zouri Bridge site

paper present the comparison between FE predicted results and the corresponding field test measurements for individual soil layers for further verification of the FE model. The subsurface soil was divided into seven soil layers for test pile 3 (TP3) site in Bayou Lacassine, which mainly consist of clayey soils. Test pile TP3 was a 22.9 m long square PPC pile with a width of 76.2 cm, which was driven by ICE I-46 type hammer. A total number of four DLTs (at 15 min, 1, 24 h, and 181 days after EOD), and two SLTs (at 15 and 175 days after EOD) were conducted to evaluate the pile setup behavior with time. In order to study setup for individual soil layers, the test pile was instrumented with vibrating wire strain gages (VWSG) installed in the soil strata boundaries to measure the side resistance for each soil layer (Hauque et al. 2016). The VWSG measurements were used to calculate pile resistance corresponded to each soil layer in the SLTs, and the resistance distributions obtained from Case Pile Wave Analysis Program (CAPWAP) were used in DLTs. The values of pile shaft resistances corresponding to the individual soil layers were extracted from results of the FE model, and were compared with the values determined from field measurements. Figure 6 presents the comparison between the field measured and FE predicted values of side resistances for the different soil layers. The figure clearly demonstrates that the FE model adopted in this study is able to

accurately predict the side resistance for individual soil layers along the pile shaft.

7 FE Parametric Study

After verification of the adopted numerical simulation technique using Bayou Zouri site and individual soil layers in Bayou Lacassine site, a similar FE pile model with dimension of 70 cm diameter and 20 m length was selected for use in the FE parametric study. The model pile was installed numerically in a soil body consisting of three layers of cohesive soils. The middle soil layer was selected to conduct the parametric study to evaluate setup of the pile side resistance, R_s . The two other layers (top and bottom) were separated from the soil domain to reduce the soil top surface boundary and the pile tip effects, respectively. Pile installation, and the following setup were simulated using the abovementioned steps.

In order to evaluate pile-soil setup behavior for different soils, the values of setup factor A that was introduced by Skov and Denver (1988) were determined for individual soil layers using the numerical simulation. The values of side resistance, R_s , for the pile segment located adjacent to the soil layer 2 were evaluated at four different times after EOD ($t = 1, 10, 100$ and 1000 days), which were obtained from the numerical simulation, at different times after EOD. They were used to calibrate the following equation:

$$\frac{R_s}{R_{s0}} = A \log\left(\frac{t}{t_0}\right) + 1 \quad (6)$$

In this study, the value of R_{s0} was considered to be the pile resistance at time $t_0 = 1$ day. Therefore, the setup factor A represent the slope of best fit line applied to the four points corresponded to $t = 1, 10, 100$ and 1000 days, which is forced to have an intercept value of 1. The FE parametric study was performed by assigning different soil properties to the layer 2, while the properties of other soil layers remained in a reasonable range. A total of 104 different soil properties of individual soil layers were collected from soil borings and/or obtained from in situ piezocone Penetration Tests (PCPT) for sites that consist of cohesive soils. The selected soil properties for the FE parametric study are undrained shear strength (S_u), soil plasticity index (PI), coefficient of consolidation (C_v),

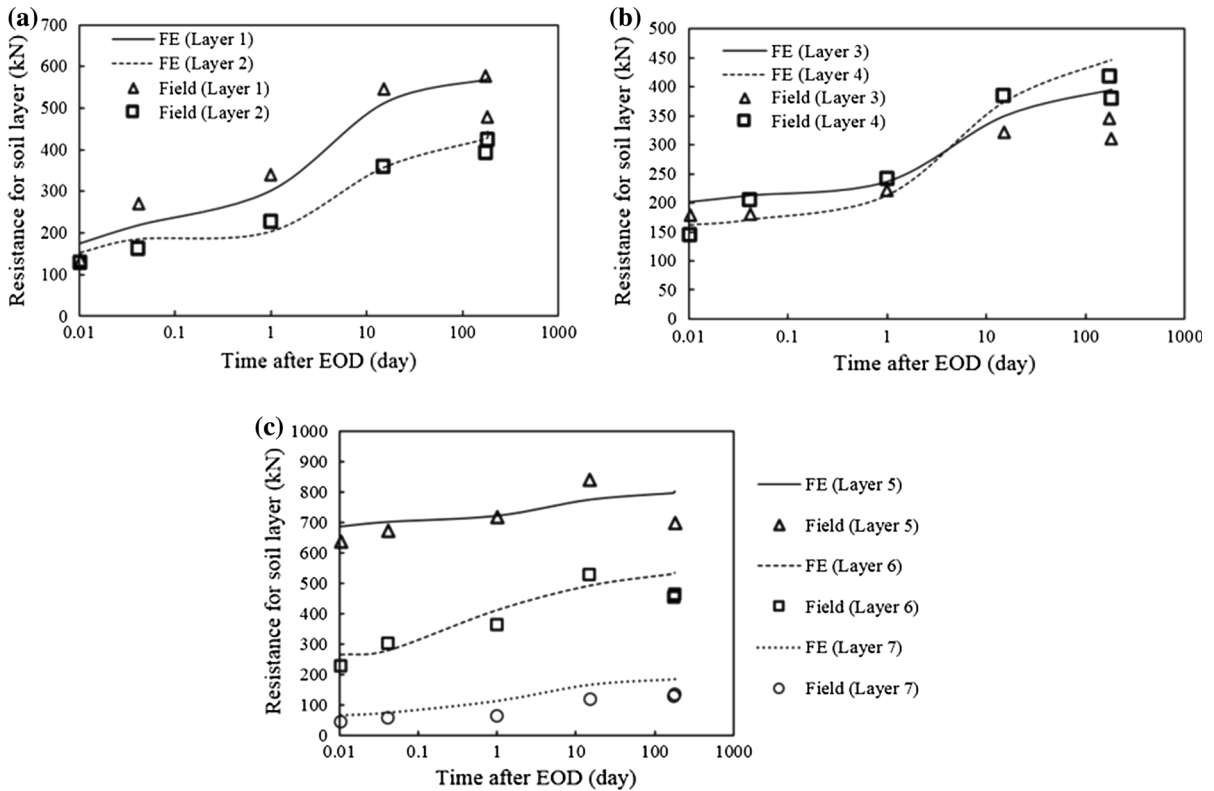


Fig. 6 Verification of FE model with comparison with field measurement of resistance of individual soil layers

Table 2 Statistical analysis of the selected properties for parametric study

Statistic	PI	S_u (tsf)	C_v (ft^2/day)	S_r	OCR
Minimum	0.10	0.07	0.003	1.00	0.35
Maximum	0.84	4.41	4.62	13.00	12.00
Range	0.80	4.34	4.62	12.00	11.75
Average	0.35	0.64	0.35	5.18	2.26
SD	0.12	0.67	0.81	2.79	2.57

sensitivity ratio (S_r), and over-consolidation ratio (OCR). The properties PI, S_r and OCR are unit-less; however, the unit used for S_u is tsf and for C_v is ft^2/day in this study. Table 2 presents a summary for statistical analysis of the soil properties.

The FE model was run for each set of soil at four different time ($t = 1, 10, 100$ and 1000) after EOD. Each run yielded a point representing the value of the pile side resistance, R_s , that corresponds to the

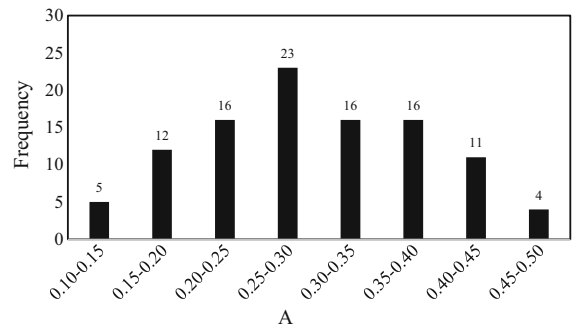


Fig. 7 Frequency histogram for setup factor A obtained from numerical simulation

setup time. The A factors were then obtained for all the 104 different individual soil layers by adopting the best-fitted line to these points and calculating the slope (A value). The frequency histogram representing the A factor obtained from FE parametric study is shown in Fig. 7.

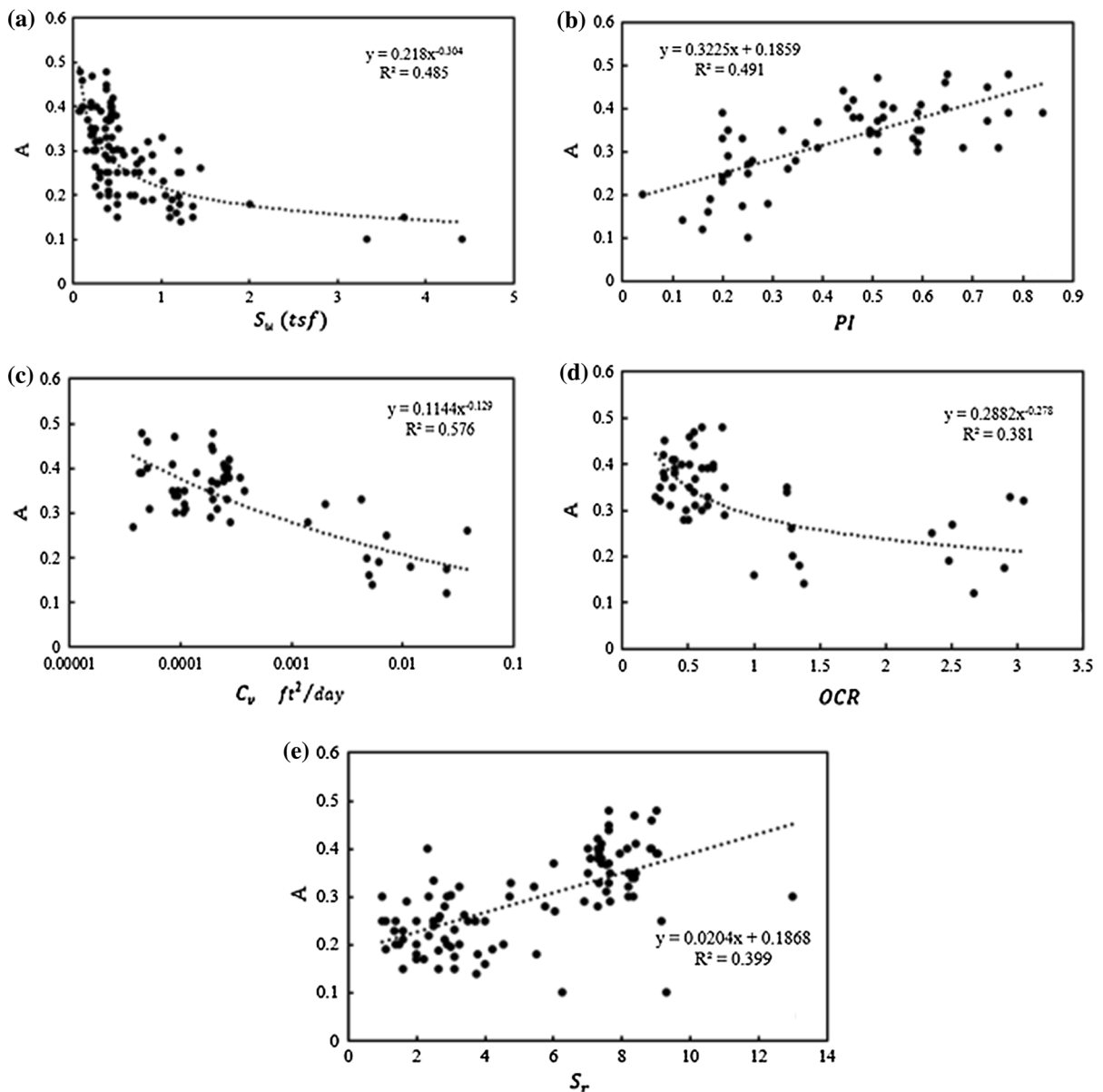


Fig. 8 Relation between setup factor A and soil properties

8 Effect of Soil Properties on Setup Factor A

In order to develop a correlation between the A factor and different soil properties, the corresponding values for A and each soil property were first drawn in graphical forms as shown in Fig. 8. The best-fit curves and the corresponding R^2 are also presented in Fig. 8.

This figure indicates that the A is directly proportional with the soil plasticity index PI and sensitivity ratio, S_r , and inversely proportional with the soil shear strength, S_u , consolidation coefficient, C_v , and over-consolidation ratio, OCR . These trends between A and soil properties will be used as guidance to conduct regression analysis in the next section.

9 Regression Analysis

Regression analyses had been extensively used to develop correlations between the dependent and independent variables when rational sets of data are available. In this study, multivariable nonlinear regression analyses were performed to establish a rational correlation between the setup factor A and the selected soil properties (i.e., PI , S_{ur} , C_v , S_r and OCR). The soil properties for parametric study, which are used as variables in the regression analysis, were initially selected based on engineering judgment. However, it is necessary to evaluate the significance level for each independent variable, which requires applying an appropriate correlation technique before including any variable in the regression model. In order to evaluate the significance level of each parameter, the statistical P values were obtained using T test, and their magnitudes were compared with the acceptance significance level criteria ($\alpha = 0.05$). P value represents the significance level within a statistical hypothesis test, and it indicates the probability of the occurrence of a given event. Stepwise evaluation procedures were applied to examine the significance level of all independent variables and the results showed that all the five selected variables have $\alpha < 0.05$. Therefore, all five variables are considered significant and will be included in the regression analysis.

The regression analysis was performed in four phases: In the first phase, the setup factor A was related to the soil shear strength, S_{ur} , and the plasticity index, PI . These two parameters were selected because of their effectiveness and availability in soil borehole logs. Nonlinear regression analysis was conducted using statistical analysis system (SAS) and curveexpert professional (CE-P) softwares. The later one was used because it is able to perform nonlinear regression for several models simultaneously. Several candidate models were selected and offered in the nonlinear regression analysis based on the rational relations exist between A and the independent variables (Fig. 8). In the second phase of regression analysis, the coefficient of consolidation C_v was first added as a third independent variable. The OCR then replaced C_v , and regression analyses were repeated. The C_v and OCR variables have inverse relation with the setup factor, A , therefore they were placed at the denominator of the proposed fractional models in the regression analyses. In the third

phase, the regression analyses were performed using four independent variables, namely, PI , S_{ur} , C_v and OCR. Regression analyses were conducted based on reasonable relation between each independent variable and the setup factor A . Finally, in the fourth phase, all the five independent variables including PI , S_{ur} , C_v , OCR and S_r were implemented in the regression analysis. Several sets of regression analyses were performed to evaluate the different proposed models, and those with the best correlation and least error of prediction were selected. The final selected models were arranged in three different sets of equations that relate the setup factor A to the corresponding soil properties that were specified as independent variables in the regression analyses. Set-1, which is shown in Table 3 presents the set of fractional relation obtained between the A factor and the different soil variables. Tables 4 and 5 present the set-2 and set-3 of correlation models, which have exponential and power relation between the A factor and different soil variables, respectively. In the tables the values R^2 represents the pseudo correlation of correlation R^2 since the actual values for it is not directly reachable in the nonlinear regression analysis. In addition, the cross-validated standard error of prediction (CVSEP) and cross-validated average error of prediction (CVAEP) were added to these tables in order to clarify the level of error in each model. External evaluation technique was adopted on the data to obtain CVSEP and CVAEP values. This technique was achieved from application of the regression equations of these tables (which were obtained based on 67 % randomly selected data out of all data) to the remained 33 % data out of all data, which yielded a value for predicted setup factor, \hat{A} . These errors were calculated based on the variation of the externally predicted \hat{A} from the A values obtained directly from numerical simulation, using the following equations:

$$CVSEP = \sqrt{\sum \frac{(\hat{A} - A)^2}{n}} \quad (7a)$$

$$CVAEP = \sum \left| \frac{(\hat{A} - A)}{n} \right| \quad (7b)$$

In Eq. 7a, 7b, $n = 34$ (or $104 \times 33 \% = 34$) representing number of data used to perform the external evaluation. The results of regression analyses,

Table 3 Regression models set 1

Model no.	Number of variables	Dependent variables	Model description	R^2	CVSEP	CVAEP
1	5	PI, S_u , C_v , OCR and S_r	$A = 0.82 \frac{(PI \times S_r)^{0.22} + 0.37}{(S_u \times C_v \times OCR)^{0.40} + 3.69}$	0.73	0.0412	0.0320
2	4	PI, S_u , C_v and OCR	$A = 0.28 \frac{PI^{0.67} + 1.44}{(S_u \times OCR \times C_v)^{0.19} + 1.28}$	0.69	0.0476	0.0397
3	3	PI, S_u and C_v	$A = 0.34 \frac{PI^{0.66} + 0.97}{(S_u \times C_v)^{0.22} + 1.26}$	0.65	0.0542	0.0449
4	3	PI, S_u and OCR	$A = 0.43 \frac{PI^{0.61} + 1.28}{(S_u \times OCR)^{0.35} + 1.82}$	0.67	0.0498	0.0415
5	2	PI and S_u	$A = 0.76 \frac{PI + 0.96}{S_u^{1.14} + 2.96}$	0.62	0.0556	0.0493

Table 4 Regression Models Set 2

Model no.	Number of variables	Dependent variables	Model description	R^2	CVSEP	CVAEP
1	5	PI, S_u , C_v , OCR and S_r	$A = 0.21 \times e^{0.7PI - 0.2S_u - 0.07C_v - 0.03OCR + 0.04S_r}$	0.68	0.0539	0.0437
2	4	PI, S_u , C_v and OCR	$A = 0.27 \times e^{0.7PI - 0.2S_u - 0.07C_v - 0.03OCR}$	0.65	0.0534	0.0442
3	3	PI, S_u and C_v	$A = 0.26 \times e^{0.7PI - 0.2S_u - 0.07C_v}$	0.63	0.0563	0.0469
4	3	PI, S_u and OCR	$A = 0.27 \times e^{0.7PI - 0.2S_u - 0.03OCR}$	0.65	0.0558	0.0464
5	2	PI and S_u	$A = 0.25 \times e^{0.7PI - 0.2S_u}$	0.61	0.0578	0.0483

Table 5 Regression Models Set 3

Model no.	Number of variables	Dependent variables	Model	R^2	CVSEP	CVAEP
1	5	PI, S_u , C_v , OCR and S_r	$A = 0.22 \left(\frac{PI \times S_r}{S_u \times OCR \times C_v} \right)^{0.06}$	0.68	0.0471	0.0395
2	4	PI, S_u , C_v and OCR	$A = 0.24 \left(\frac{PI \times S_r}{S_u \times OCR \times C_v} \right)^{0.07}$	0.66	0.0509	0.0423
3	3	PI, S_u and C_v	$A = 0.23 \left(\frac{PI}{S_u \times C_v} \right)^{0.08}$	0.60	0.0549	0.0458
4	3	PI, S_u and OCR	$A = 0.31 \left(\frac{PI}{S_u \times OCR} \right)^{0.12}$	0.66	0.0517	0.0467
5	2	PI and S_u	$A = 0.31 \left(\frac{PI}{S_u} \right)^{0.18}$	0.59	0.0585	0.0482

as presented in Tables 3, 4 and 5, indicate that R^2 increases, while CVSEP and CVAEP decrease with increasing number of independent soil variables. By comparing, the values of R^2 , CVSEP and CVAEP presented in the last two columns of these tables, the reader can realize that the correlation equation in these three sets have almost the same level of accuracy. Furthermore, each set of

models presented in Tables 3, 4, and 5 includes five regression models, which are ranked from 1 to 5 based on the corresponding value of errors. The model number 1 in each set represents the best equation to estimate the setup factor A , which can be used to estimate the A values if all the required soil properties (i.e., PI, S_u , C_v , S_r and OCR) are available. However, in the case not all the required soil properties are

available, the reader can use models 2–5 of each set with acceptable accuracy to estimate the setup factor *A*, depending on availability of the soil properties. This concept can be applied in order to evaluate the three sets of models presented in Tables 3, 4 and 5.

10 Verification of the Proposed Models

To verify the proposed regression models in Tables 3, 4 and 5, the information of soil properties and setup values for additional sites were collected from literature (e.g., Titi and Wathugala 1999; Augustesen 2006; Ng 2011). The selected additional sites were not included in the database used in parametric study to develop the regression models. Table 6 presents the additional selected sites used for verification and the corresponding soil properties as well as the measured *A* factor. In this table, the *A* values were back-calculated from static and dynamic field load tests. Each set of models (set-1, set-2, and set-3) was used to calculate the setup factor *A* based on the availability of the soil properties presented in Table 6. This means that model 1 of each set was used to predict the *A* if all

soil properties are available, while models 2–5 were used if some values of the soil properties were not available. Figure 9 presents the comparison between the predicted *A* using the proposed regression models of each set and the back-calculated *A* values from static and dynamic load tests. The figure indicates that the three sets of models proposed in Tables 3, 4 and 5 are able to reasonably estimate the soil setup behavior, especially for soils with *A* values greater than 0.10. The figure also demonstrated that the predictions of *A* values using the models set-1 (Fig. 9a) are slightly better than the predictions of the other two model sets (Fig. 9b, c).

11 Summary and Conclusions

In this study, pile setup phenomenon, which usually occurs in pile driven in saturated cohesive soils, was studied using FE parametric study. Pile installation and the following setup phenomenon were modeled using volumetric cavity expansion applied at the soil boundary followed by shearing step. The pile shaft resistance was then obtained by applying an additional

Table 6 Site information used for verification of proposed regression models

No.	Site name	Reference	PI	<i>S_u</i> (tsf)	<i>C_v</i> ($\frac{ft^2}{day}$)	OCR	Field measured <i>A</i>
1	Sabin River	Titi and Wathugala (1999)	0.73	0.24	0.01	1	0.45
2	Houston		0.31	1.09	–	8.1	0.23
3	St. Alban		0.21	0.19	–	4.6	0.46
4	Drammen		0.21	0.21	–	1.1	0.34
5	Canons park		0.47	0.96	–	8.4	0.22
6	Bothkenner		0.40	0.17	–	2.9	0.33
7	Drammen Stasjon	Augustesen (2006)	0.22	0.82	–	1.2	0.32
8	Nitsund		0.16	0.68	–	14	0.16
9	Sky-Edeby		0.40	0.11	–	4	0.32
10	Haga		0.18	0.41	–	7.3	0.22
11	Algade		0.25	1.34	–	9.7	0.18
12	Motorvegbru		0.25	0.65	–	1.1	0.32
13	Sumatra		0.40	0.35	–	2.3	0.28
14	Cowden		0.15	1.36	–	25.2	0.16
15	ISU2	Ng (2011)	0.15	0.89	1.81	1	0.10
16	ISU3		0.10	1.24	1.44	1.6	0.05
17	ISU4		0.15	1.45	1.30	1.2	0.15
18	ISU5		0.18	1.65	1.30	1.3	0.07
19	ISU6		0.09	1.84	1.22	1.5	0.10

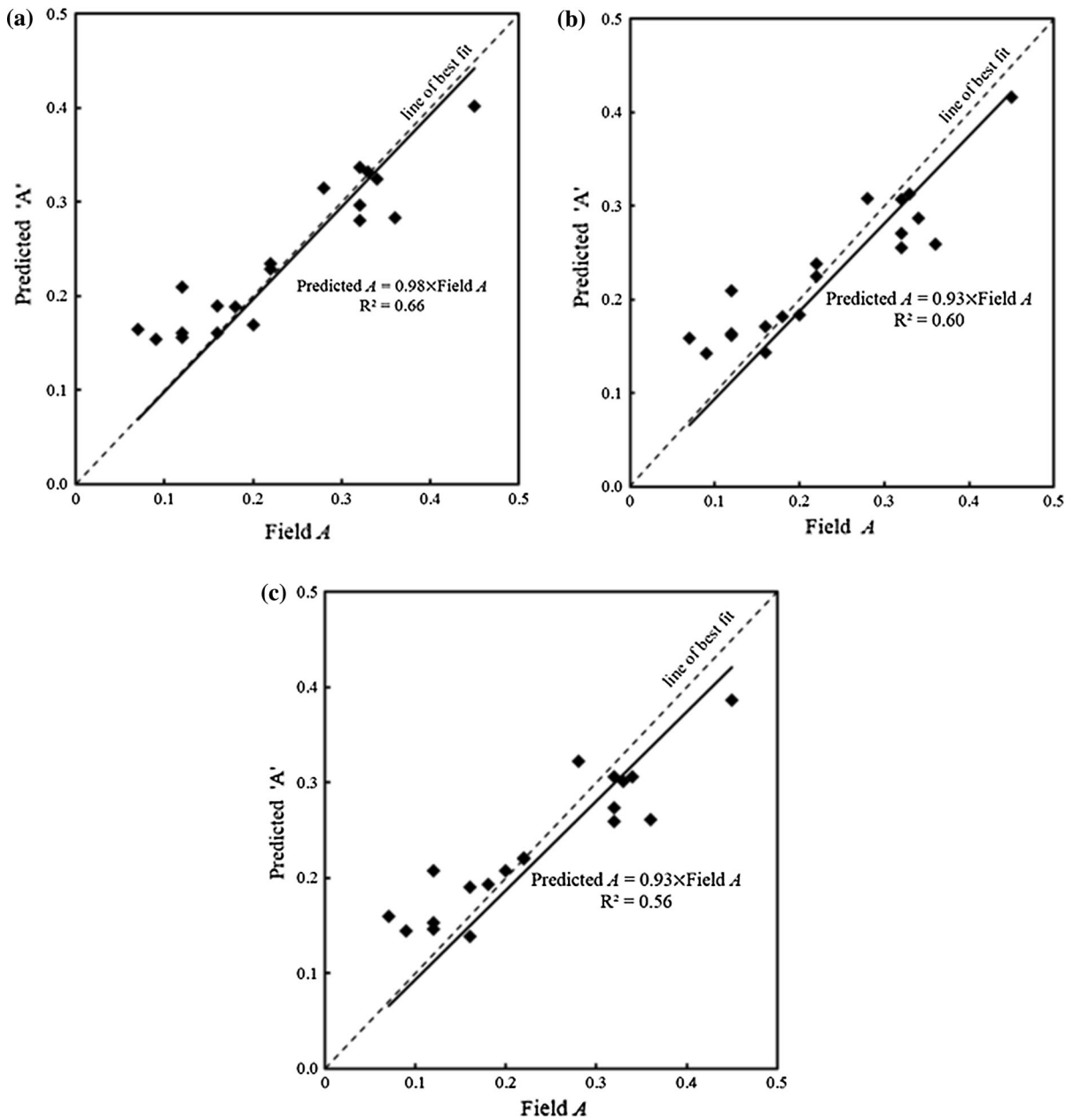


Fig. 9 Verification of proposed regression models in order to predict A factor: **a** models set-1, **b** models set-2, and **c** models set-3

vertical shear at different times after EOD. In order to validate the FE numerical simulation, a full-scale pile installation case study was first simulated using FE technique, and the pile shaft capacities at different time after EOD were obtained. Another full-scale pile installation case study including seven individual soil layers was then selected to verify the numerical simulation. After verification of the proposed

numerical model, an extensive parametric study was conducted to investigate the effect of different soil properties on the setup phenomenon. The setup factor A that was introduced by Skov and Denver (1988) was considered as the main representative of the soil setup behavior. The numerical simulation was performed, and pile installation in saturated cohesive soil and the following setup were simulated at different times after

EOD to obtain the setup factor A . The anisotropic modified cam-clay model was adopted to describe the behavior of saturated cohesive soil. Both the dissipation of excess pore water pressure (consolidation setup) and the soil disturbance during pile installation and the following strength regaining over time (thixotropic setup) were considered in the FE model to evaluate the setup behavior for individual soil layers in this study. Over 100 different soil properties of individual soil layers including the soil plasticity index (PI), undrained shear strength (S_u), vertical coefficient of consolidation (C_v), sensitivity ratio (S_r), and over-consolidation ratio (OCR) were collected from literature to perform FE parametric study. In order to achieve the rational relations between the setup factor A and the different soil properties, several multivariable nonlinear regression analysis were performed using the statistical analysis system (SAS) and curve-expert professional (CE-P) softwares. Based on the results of this study, the following conclusions can be drawn:

- The numerical simulation technique adopted in this paper using volumetric cavity expansion in FE is able to predict the shaft resistance of driven piles and to evaluate the pile setup phenomenon appropriately.
- The FE parametric study indicated that the setup factor A is directly proportional to the soil plasticity index, PI, and sensitivity ratio, S_r , and inversely proportional to the soil shear strength, S_u , vertical consolidation coefficient, C_v , and over-consolidation ratio, OCR.
- Statistical analyses using the T-test and the corresponding P-values showed that all the selected five soil properties were significant in the regression analysis for evaluating setup behavior.
- Regression analyses were conducted to develop analytical models to estimate the setup factor A as a function of selected soil properties. The regression analyses were performed in four different phases, in which different numbers of soil properties were selected as independent variables in each phase. The conducted analyses yielded several regression models; however, the most accurate models were selected and grouped into three sets of equations (set-1, set-2 and set-3) based on the correlation coefficient and least square of prediction errors.
- Verification of the three regression model sets, using data available in the literature for an additional 19 different sites, indicated that all the three models were able to reasonably estimate the setup behavior of individual cohesive soil layers; especially for soils with the setup factor A greater than 0.10. The models of set-1 demonstrate better accuracy than the models of set-2, which are a little more accurate than the models in set-3 in estimating the setup factor A .

Acknowledgments This research is funded by the Louisiana Transportation Research Center (LTRC Project No. 11-2GT) and Louisiana Department of Transportation and development (LADOTD) [State Project No. 736-99-1732]. The authors appreciate Gavin Gautreau for providing the field test data for the projects.

References

- Abu-Farsakh M, Tumay M, Voyiadjis G (2003) Numerical parametric study of piezocone penetration test in clays. *Int J Geomech* 3(4):170–181
- Abu-Farsakh M, Rosti F, Souri A (2015) Evaluating pile installation and subsequent thixotropic and consolidation effects on setup by numerical simulation for full-scale pile load tests. *Can Geotech J* 52:1–13
- Augustesen AH (2006) The effect of time on soil behavior and pile capacity. Ph.D. dissertation. Department of Civil Engineering, Aalborg University, Denmark
- Barnes HA (1997) Thixotropy—a review. *Int J Non-Newton Fluid Mech* 70:1–33
- Bullock PJ, Schmertmann JH, McVay MC, Townsend FC (2005) Side shear setup. II: results from Florida test piles. *J Geotech Geoenviron Eng* 131(3):301–303
- Chakraborty T, Salgado R, Loukidis D (2013) A two-surface plasticity model for clay. *Comput Geotech* 49:170–190
- Chen Q, Haque MN, Abu-Farsakh M, Fernandez BA (2014) Field investigation of pile setup in mixed soil. *Geotech Test J* 37(2):268–281
- Dafalias YF (1987) An anisotropic critical state clay plasticity model. *Constitutive laws for engineering materials: theory and applications*. Elsevier, Amsterdam, pp 513–521
- Elias MB (2008) Numerical simulation of pile installation and setup. Ph.D. dissertation, The University of Wisconsin, Milwaukee, WI
- Fakharian K, Attar IH, Haddad H (2013) Contributing factors on setup and the effects on pile design parameter. In: *Proceeding of the 18th international conference on soil mechanics and geotechnical engineering*, Paris
- Haque MN, Abu-Farsakh M, Chen Q, Zhang Z (2014) A case study on instrumentation and testing full-scale test piles for

- evaluating set-up phenomenon. Transportation research record. J Transp Res Rec, 2462 Soil Mechanics, pp 37–47
- Haque MN, Abu-Farsakh M, Zhang Z, Okeil A (2016) Evaluate pile set-up for individual soil layers and develop a model to estimate the increase in unit side resistance with time based on PCPT data. Transportation research record: J Transp Res Rec (in press)
- Karlsrud K, Clausen CJF, Aas PM (2005) Bearing capacity of driven piles in clay, the NGI approach. In: Proceeding of international symposium on frontiers in offshore geotechnics, Perth Sept. 2005, A.A. Balkema Publishers, pp 775–782
- Khan L, Decapite K (2011) Prediction of pile set-up for Ohio soils. Federal Highway Administration Report FHWA/OH-2011/3, Ohio Department of Transportation, Columbus, Ohio, USA, p 34
- Konard JM, Roy M (1987) Bearing capacity of friction pile in marine clay. Geotechnique 37(2):163–175
- Mitchell JK (1960) Fundamentals aspects of thixotropy in soils. J Soil Mech Found Des 86:19–52
- Ng KW (2011) Pile setup, dynamic construction control, and load and resistance factor design of vertically-loaded steel HPiles. Graduate theses and dissertations. Paper 11924
- Ng KW, Roling M, AbdelSalam SS, Suleiman MT, Sritharan S (2013) Pile setup in cohesive soil. I: experimental investigation. J Geotech Geoenviron Eng 139(2):199–209
- Randolph MF, Wroth CP (1979) Driven piles in clay: effects of installation and subsequence consolidation. Int J Geotech 29(4):361–393
- Rosti F, Abu-Farsakh M (2015) Numerical simulation of pile installation and setup for Bayou Laccasine Site. Geotechnical Special publication No. 256. IFCEE2015, pp 1152–1161
- Salgado R (2008) Engineering of foundations. Mc Graw-Hill, New York
- Shao C (1998) Implementation of DSC model for dynamic analysis of soil structure interaction problems. Ph.D. Dissertation, Dept. of Civil Engineering, University of Arizona, Tucson, Arizona
- Skov R, Denver H (1988) Time-dependence of bearing capacity of piles. In: Fellenius BH (ed) Proceedings of 3rd international conference on the application of stress-wave theory to piles, Ottawa, Ontario, Canada, 879–888
- Teh CI, Houlsby GT (1991) An analytical study of the cone penetration test in clay. Geotechnique 41(1):17–34
- Titi HH, Wathugala GW (1999) Numerical procedure for predicting pile capacity setup/freeze. J Transp Res Rec 1663:23–32
- Walker J, Yu HS (2006) Adaptive finite element analysis of cone penetration in clay. Acta Geotech 1:43–57
- Wathugala GW (1990) Finite element dynamic analysis of nonlinear porous media with application to the piles in saturated clay. Ph.D. dissertation, Department of Civil Engineering, University of Arizona, Tucson, Arizona